

## Redox Control of Photoinduced Electron Transfer in Axial Terpyridoxy Porphyrin Complexes

Prashanth Kumar Poddutoori,<sup>†,‡</sup> Premaladha Poddutoori,<sup>‡</sup> Bhaskar G. Maiya,<sup>‡,⊥</sup> Thazhe Kootteri Prasad,<sup>‡</sup> Yuri E. Kandrashkin,<sup>†,§</sup> Sergei Vasil'ev,<sup>||</sup> Doug Bruce,<sup>||</sup> and Art van der Est<sup>\*,†</sup>

Departments of Chemistry and Biological Sciences, Brock University, 500 Glenridge Avenue, St. Catharines, Ontario L2S 3A1, Canada, School of Chemistry, University of Hyderabad, Hyderabad 500 046, India, and Zavoisky Physical-Technical Institute, 10/7 Sibirsky Tract, Kazan 420029, Russian Federation

Received December 21, 2007

The photophysical properties of axial-bonding types (terpyridoxy)aluminum(III) porphyrin (Al(PTP)), bis(terpyridoxy)tin(IV) porphyrin (Sn(PTP)<sub>2</sub>), and bis(terpyridoxy)phosphorus(V) porphyrin ([P(PTP)<sub>2</sub>]<sup>+</sup>) are reported. Compared with their hydroxy analogues, the fluorescence quantum yields and singlet-state lifetimes were found to be lower for Sn(PTP)<sub>2</sub> and [P(PTP)<sub>2</sub>]<sup>+</sup>, whereas no difference was observed for Al(PTP). At low temperature, all of the compounds show spin-polarized transient electron paramagnetic resonance (TREPR) spectra that are assigned to the lowest excited triplet state of the porphyrin populated by intersystem crossing. In contrast, at room temperature, a triplet radical-pair spectrum that decays to the porphyrin triplet state with a lifetime of 175 ns is observed for [P(PTP)<sub>2</sub>]<sup>+</sup>, whereas no spin-polarized TREPR spectrum is found for Sn(PTP)<sub>2</sub> and only the porphyrin triplet populated by intersystem crossing is seen for Al(PTP). These results clarify the role of the internal molecular structure and the reduction potential for electron transfer from the terpyridine ligand to the excited porphyrin. It is argued that the efficiency of this process is dependent on the oxidation state of the metal/metalloid present in the porphyrin and the reorganization energy of the solvent.

## Introduction

The oxidation of water during photosynthesis is one of the most important chemical processes known. The oxygen that evolved in this process dramatically altered the composition of the earth's atmosphere and is vital to many living organisms. Despite the importance of this process and many years of study, the mechanism by which water is oxidized is still a subject of intense debate. (See McEvoy and Brudvig<sup>1</sup> for a recent review.) One approach to this problem has been to construct model compounds that mimic features of the water-splitting complex.<sup>2–12</sup> Such biomimetic compounds are also of interest as potential catalysts for other oxidation reactions.<sup>13</sup> The majority of these catalysts reported in the

literature are either bi- or tetranuclear Mn complexes containing  $\mu$ -oxo bridges between the Mn atoms by analogy to the emerging structure of the oxygen-evolving complex (OEC) of photosystem II (PS II).<sup>12</sup> Similar structures containing Ru in place of Mn have also been investigated. See Kurz et al.<sup>2</sup> for a recent comparison of the catalytic activity of several such complexes. In PS II, the OEC is activated by four successive photo-oxidations, after which it is able to oxidize two water molecules, extracting four electrons and releasing an oxygen molecule and four protons in the process. To date, this process has not been modeled successfully in an artificial system, and chemical oxidation is needed to activate the catalysts. However, recently, some progress toward this goal has been made by demonstrating

\* To whom correspondence should be addressed. E-mail: avde@brocku.ca.

<sup>†</sup> Brock University, Department of Chemistry.

<sup>‡</sup> University of Hyderabad.

<sup>§</sup> Zavoisky Physical-Technical Institute.

<sup>||</sup> Brock University, Department of Biological Sciences.

<sup>⊥</sup> Deceased.

(1) McEvoy, J. P.; Brudvig, G. W. *Chem. Rev.* **2006**, *106*, 4455–4483.

(2) Kurz, P.; Berggren, G.; Anderlund, M. F.; Styring, S. *Dalton Trans.* **2007**, 4258–4261.

(3) Yagi, M.; Narita, K.; Maruyama, S.; Sone, K.; Kuwabara, T.; Shimizu, K. *Biochim. Biophys. Acta* **2007**, *1767*, 660–665.

(4) Abuabara, S. G.; Cady, C. W.; Baxter, J. B.; Schmuttenmaer, C. A.; Crabtree, R. H.; Brudvig, G. W.; Batista, V. S. *J. Phys. Chem. C* **2007**, *111*, 11982–11990.

that the photo-oxidation of Mn is possible in complexes in which the Mn center is linked to a Ru-bipyridine complex<sup>9,12,14</sup> or a TiO<sub>2</sub> nanoparticle.<sup>4</sup> In PS II, the photo-oxidation of the OEC occurs as a result of light-induced electron transfer, which generates the highly oxidizing radical cation P<sub>680</sub><sup>+</sup>. The challenge in designing artificial systems is to find an appropriate model for this species. It is well established that P<sub>680</sub> is a chlorophyll dimer that is similar to the primary electron donors in other types of reaction centers. However, its redox potential has been tailored for water oxidation by the local environment.<sup>15</sup> For artificial complexes, there is no surrounding protein, and thus other ways of tuning the redox potential of the photosensitizer must be sought.

There is a rich literature of porphyrin-based donor–acceptor (D–A) systems as models for the electron-transfer cofactors in photosynthesis.<sup>16–18</sup> However, despite their structural similarity to chlorophylls, porphyrins have not been widely studied as possible sensitizers for model water-splitting complexes. Instead, Ru(bpy)<sub>3</sub><sup>2+</sup> has generally been used because it provides an easy route to the necessary combination of oxidation potential and optical properties.<sup>12,14</sup> However, this comes at the expense of a realistic model for P<sub>680</sub>. Axially bound P porphyrins have been studied recently as sensitizers involved in oxidation, such as dye-sensitized semiconductor solar cells<sup>19</sup> that use hole injection and as potential photodynamic therapy agents<sup>20–22</sup> that cause light-induced oxidation of DNA. Moreover, they have a number of features in common with the chlorophylls of P<sub>680</sub>,

including a similar tetrapyrrole structure and axial ligation.<sup>23–25</sup> On the basis of these similarities, we have begun exploring the possibility of using a P porphyrin as a model for P<sub>680</sub> and have reported on the energy and electron-transfer properties of a series of P porphyrin complexes in which terpyridine was covalently attached in the axial position to provide a metal-binding site.<sup>26,27</sup> These studies<sup>26,27</sup> suggest that the excitation of the porphyrin may lead to radical-pair formation by electron transfer from terpyridine to the excited porphyrin. We hypothesized that this process is promoted by the high oxidation state of P. Here, we test this hypothesis and investigate the possibility of redox control of the electron transfer by introducing Al(III) and Sn(IV) to the porphyrin to create a series of analogous complexes with different oxidation numbers for the metal/metalloid. The structures of the complexes Al(PTP), Sn(PTP)<sub>2</sub>, and [P(PTP)<sub>2</sub>]<sup>+</sup> (PTP is phenylterpyridine) are shown in Figure 1.

Electrochemical and steady-state spectroscopic measurements indicate that as expected the oxidation number of the central metal/metalloid correlates with the reduction potential of the porphyrin and should therefore provide a way of controlling the electron-transfer properties of the complex. This is confirmed by time-resolved fluorescence data and the spin polarization patterns obtained from transient electron paramagnetic resonance (TREPR), which show evidence of electron transfer only when the reduction potential of the porphyrin is sufficiently positive. The prospects of using these systems as photosensitizers for Mn complexes will be discussed.

## Experimental Section

**Synthesis.** Compounds Al(PTP), Sn(PTP)<sub>2</sub>, and [P(PTP)<sub>2</sub>]<sup>+</sup> were synthesized using methods described in the Supporting Information section. The structures of the compounds were confirmed by <sup>1</sup>H NMR and mass spectral data.

**X-ray Crystallography.** The structure of Sn(PTP)<sub>2</sub> was also confirmed by X-ray crystallography. The scattering data were collected at 100(2) K on a Bruker SMART APEX CCD X-ray diffractometer using graphite-monochromated Mo K $\alpha$  radiation. The detector was placed at a distance of 4.995 cm from the crystal. The data were reduced using SAINTPLUS,<sup>28</sup> and a multiscan absorption correction using SADABS<sup>29</sup> was performed. The structure was solved using SHELXS-97,<sup>30</sup> and full-matrix least-squares refinement against *F*<sup>2</sup> was carried out using SHELXL-97.<sup>30</sup> All hydrogens were assigned on the basis of geometrical considerations and were allowed to ride upon the respective carbon atoms.

- (5) Tagore, R.; Chen, H. Y.; Zhang, H.; Crabtree, R. H.; Brudvig, G. W. *Inorg. Chim. Acta* **2007**, *360*, 2983–2989.
- (6) Anderlund, M. F.; Höglblom, J.; Shi, W.; Huang, P.; Eriksson, L.; Weihe, H.; Styring, S.; Akermark, B.; Lomoth, R.; Magnuson, A. *Eur. J. Inorg. Chem.* **2006**, *503*, 3–5047.
- (7) Borgström, M.; Shaikh, N.; Johansson, O.; Anderlund, M. F.; Styring, S.; Akermark, B.; Magnuson, A.; Hammarström, L. *J. Am. Chem. Soc.* **2005**, *127*, 17504–17515.
- (8) Huang, P.; Höglblom, J.; Anderlund, M. F.; Sun, L. C.; Magnuson, A.; Styring, S. *J. Inorg. Biochem.* **2004**, *98*, 733–745.
- (9) Wolpher, H.; Ping, H.; Borgström, M.; Bergquist, J.; Styring, S.; Sun, L. C.; Akermark, B. *Catal. Today* **2004**, *98*, 529–536.
- (10) Limburg, J.; Vrettos, J. S.; Chen, H. Y.; de Paula, J. C.; Crabtree, R. H.; Brudvig, G. W. *J. Am. Chem. Soc.* **2001**, *123*, 423–430.
- (11) Limburg, J.; Vrettos, J. S.; Liable-Sands, L. M.; Rheingold, A. L.; Crabtree, R. H.; Brudvig, G. W. *Science* **1999**, *283*, 1524–1527.
- (12) Lomoth, R.; Magnuson, A.; Sjödin, M.; Huang, P.; Styring, S.; Hammarström, L. *Photosynth. Res.* **2006**, *87*, 25–40.
- (13) Tanase, S.; Bouwman, E. *Adv. Inorg. Chem.* **2006**, *58*, 29–75.
- (14) Romain, S.; Leprêtre, J. C.; Chauvin, J.; Deronzier, A.; Collomb, M. N. *Inorg. Chem.* **2007**, *46*, 2735–2743.
- (15) Renger, G.; Holzwarth, A. R. Primary Electron Transfer. In *Photosystem II: The Light-Driven Water: Plastocyanin Oxidoreductase*; Wydrzynski, T., Satoh, K., Eds.; Springer: Dordrecht, The Netherlands, 2005; Vol. 22, pp 139–175.
- (16) Wasielewski, M. R. *Chem. Rev.* **1992**, *92*, 435–461.
- (17) Gust, D.; Moore, T. A.; Moore, A. L. *Acc. Chem. Res.* **2001**, *34*, 40–48.
- (18) Holten, D.; Bocian, D. F.; Lindsey, J. S. *Acc. Chem. Res.* **2002**, *35*, 57–69.
- (19) Borgström, M.; Blart, E.; Boschloo, G.; Mukhtar, E.; Hagfeldt, A.; Hammarström, L.; Odobel, F. *J. Phys. Chem. B* **2005**, *109*, 22928–22934.
- (20) Liu, F.; Cardolaccia, T.; Hornstein, B. J.; Schoonover, J. R.; Meyer, T. J. *J. Am. Chem. Soc.* **2007**, *129*, 2446.
- (21) Hirakawa, K.; Kawanishi, S.; Hirano, T.; Segawa, H. *J. Photochem. Photobiol., B* **2007**, *87*, 209–217.
- (22) Hirakawa, K.; Kawanishi, S.; Segawa, H.; Hirano, T. *J. Porphyrins Phthalocyanines* **2006**, *10*, 1285–1292.

- (23) Loll, B.; Kern, J.; Saenger, W.; Zouni, A.; Biesiadka, J. *Nature* **2005**, *438*, 1040–1044.
- (24) Kamiya, N.; Shen, J. R. *Proc. Natl. Acad. Sci. U.S.A.* **2003**, *100*, 98–103.
- (25) Ferreira, K. N.; Iverson, T. M.; Maghlaoui, K.; Barber, J.; Iwata, S. *Science* **2004**, *303*, 1831–1838.
- (26) Kumar, P. P.; Premaladha, G.; Maiya, B. G. *Chem. Commun.* **2005**, 3823–3825.
- (27) Kandrashkin, Y. E.; Poddutoori, P. K.; van der Est, A. *Appl. Magn. Reson.* **2006**, *30*, 605–618.
- (28) SAINTPlus; Bruker AXS, Inc.: Madison, WI, 2001.
- (29) Sheldrick, G. M. *SADABS Program for Empirical Absorption Correction of Area Detectors*; Georg-August-Universität Göttingen: Germany, 1996.
- (30) Sheldrick, G. M. *SHELXS-97 and SHELXL-97*; Georg-August-Universität Göttingen: Germany, 1997.

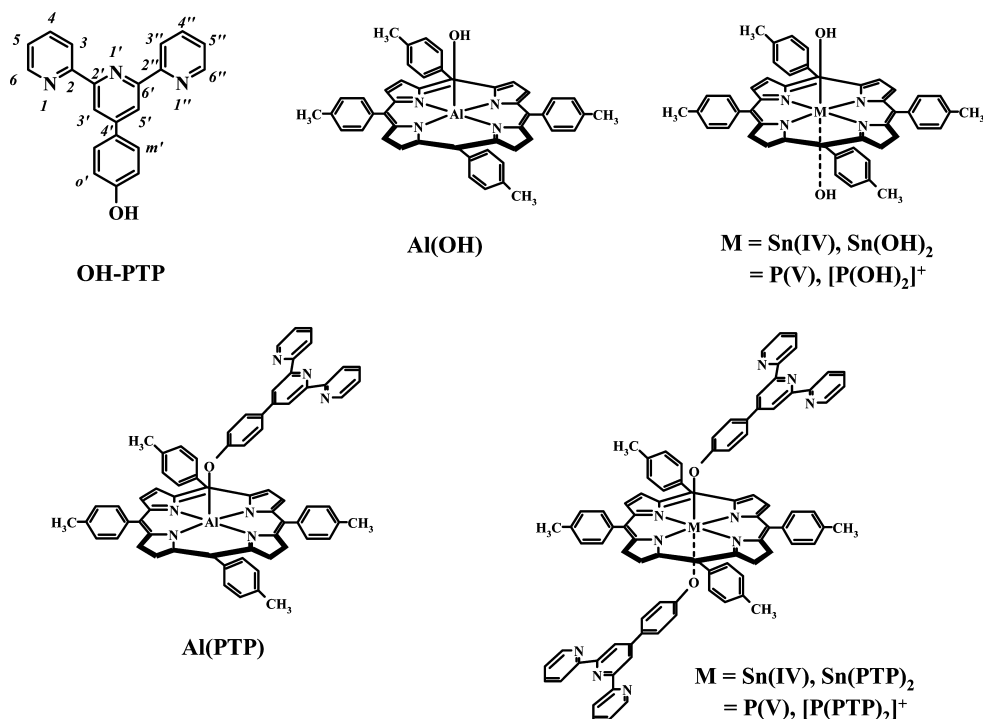


**Figure 1.** Structures and abbreviated names of the porphyrins with axially bound terpyridine as well as the corresponding hydroxy compounds.

**Electrochemistry.** Cyclic and differential pulse voltammetric experiments ( $\text{CH}_2\text{Cl}_2$ , 0.1 M tetrabutylammonium perchlorate, TBAP) were performed on a CH Instruments model CHI 620A electrochemical analyzer as detailed elsewhere (working and auxiliary electrodes are Pt; reference electrode is Ag).<sup>31–33</sup> The Fc<sup>+</sup>/Fc (Fc = ferrocene) couple was used to calibrate the redox potential values, which are reported in volts versus SCE ( $E_{1/2}(\text{Fc}^+/\text{Fc}) = 0.48$  V versus SCE in  $\text{CH}_2\text{Cl}_2$ , 0.1 M TBAP)<sup>34</sup> under our experimental conditions.

**Steady-State Ultraviolet/Visible Absorption and Fluorescence Spectroscopy.** The UV/vis spectra were recorded on a Shimadzu model UV-3101 PC UV/vis spectrophotometer. Sample concentrations ranged from  $1 \times 10^{-6}$  M, for the measurement of the porphyrin Soret band, to  $6 \times 10^{-5}$  M, for the porphyrin Q bands and terpyridine bands. Steady-state fluorescence spectra (uncorrected) were recorded using a Spex model Fluoromax-3 spectrofluorimeter. The concentrations of the fluorophores were adjusted so that the optical density (OD) at the excitation wavelength was always  $\sim 0.2$ .

**Nuclear Magnetic Resonance and Mass Spectrometry.** <sup>1</sup>H NMR spectra were recorded on a Bruker NR-400 AF-FT NMR spectrometer using  $\text{CDCl}_3$  as the solvent and tetramethylsilane (TMS) as an internal standard. The proton-decoupled <sup>31</sup>P NMR spectra were recorded on the same instrument using 85%  $\text{H}_3\text{PO}_4$  as an external standard. FAB mass spectra were recorded on a Kratos Concept 1S high-resolution E/B mass spectrometer.

**Time-Resolved Fluorescence Spectroscopy.** A time-correlated single-photon-counting apparatus utilizing a picosecond-pulsed diode laser was used to measure the porphyrin fluorescence decay. Excitation pulses were delivered at 407 nm by a picosecond diode laser (PicoQuant, PDL 800-B), 54 ps fwhm, at a repetition rate of 10 MHz. The porphyrin fluorescence was measured by a Hamamat-

su R3809 microchannel plate photomultiplier screened by a double monochromator. A single-photon-counting PC card (Becker & Hickl, SPC-730) was used for data collection. The instrument response time of the system was 80 ps.

**Transient Electron Paramagnetic Resonance Spectroscopy.** TREPR time/field data sets were recorded using a modified Bruker EPR 200D-SRC X-band spectrometer (Bruker Canada, Milton ON, Canada). The optical excitation at 532 nm was achieved by the use of 10 ns pulses from a Nd:YAG laser at a repetition rate of 10 Hz. EPR samples were prepared by dissolving the porphyrin complex under study in a liquid-crystalline solvent, E7 or 5CB (Merck), to a concentration of  $\sim 10^{-4}$  M. The solvent 5CB is *p*-(*n*-pentyl)cyanobiphenyl, whereas E7 is mixture of alkyl cyanobiphenyls, one of which is 5CB. The solutions were placed in suprasil EPR sample tubes (4 mm o.d.) and were degassed by several freeze–pump–thaw cycles and then sealed under vacuum.

## Results

Before discussing the photochemistry of the complexes, we consider some features of their physical and electronic structures.

**X-ray Structure of Sn(PTP)<sub>2</sub>·2H<sub>2</sub>O.** Two views of the X-ray structure of Sn(PTP)<sub>2</sub>·2H<sub>2</sub>O are shown in Figure 2. For clarity, the waters of crystallization have been omitted. The crystal packing and experimental details are given in the Supporting Information. As is usual for metalloporphyrins, the Sn atom lies in a center of symmetry, and the geometry around it is almost regular octahedral with the porphyrin ring forming the equatorial plane and with terpyridines at the axial positions. The two terpyridines adopt an anti arrangement with respect to each other and subtend an angle of 34.7° with respect to the porphyrin plane. The bridging phenyl group of each terpyridine ligand is oriented in a cofacial arrangement with one of the pyrrole rings of the porphyrin such that the pyrrole nitrogen is roughly at

(31) Kumar, P. P.; Premaladha, G.; Maiya, B. G. *J. Chem. Sci.* **2005**, *117*, 193–201.

(32) Reddy, D. R.; Maiya, B. G. *J. Phys. Chem. A* **2003**, *107*, 6326–6333.

(33) Poddutoori, P. K.; Poddutoori, P.; Maiya, B. G. *J. Porphyrins Phthalocyanines* **2006**, *10*, 1049–1060.

(34) Connelly, N. G.; Geiger, W. E. *Chem. Rev.* **1996**, *96*, 877–910.

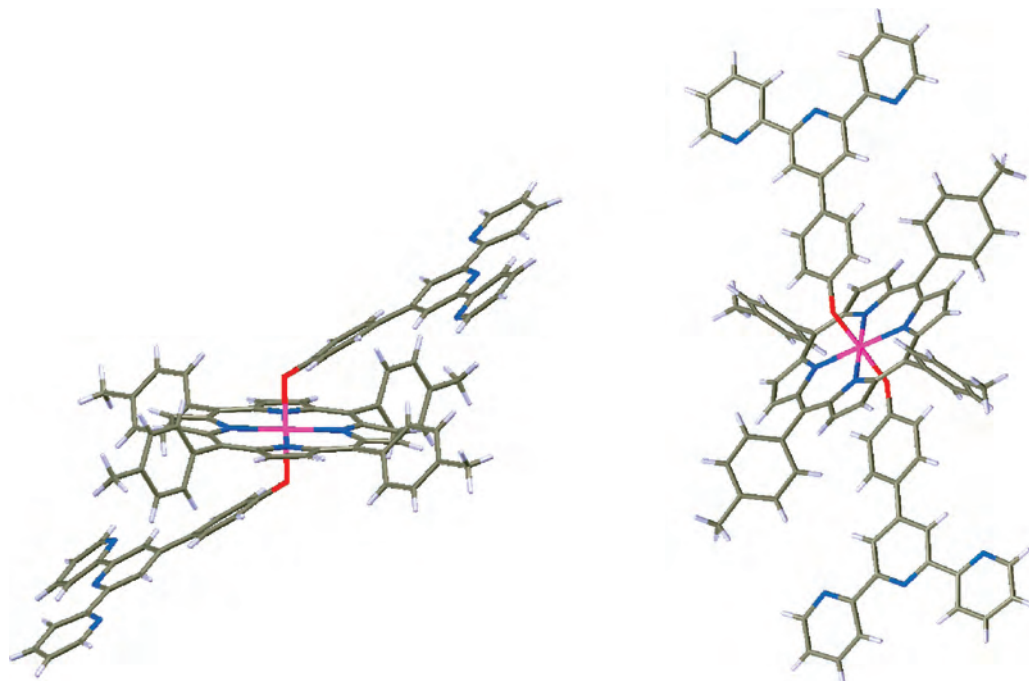


**Figure 2.** X-ray structure of  $\text{Sn(PTP)}_2 \cdot 2\text{H}_2\text{O}$  shown from two different perspectives. The solvent water molecules are not shown.

the center of the phenyl group when viewed along the normal to the porphyrin plane. This arrangement suggests that the  $\pi-\pi$  interactions between the ligands and the porphyrin could be substantial.

**Ultraviolet/Visible Spectroscopy.** The UV/vis absorption and fluorescence spectra of the complexes  $\text{Al(PTP)}$ ,  $\text{Sn(PTP)}_2$ , and  $[\text{P(PTP)}_2]^+$  and the corresponding hydroxy analogues  $\text{Al(OH)}$ ,  $\text{Sn(OH)}_2$ , and  $[\text{P(OH)}_2]^+$  are shown in Figure 3. The absorbance maxima ( $\lambda_{\text{max}}$ ) and corresponding molar extinction coefficients ( $\epsilon$ ) in different solvents are tabulated in the Supporting Information section.

**Terpyridine–Porphyrin Interactions.** The absorbance spectra in Figure 3 (solid curves) show that for  $\text{Al(PTP)}$  and  $\text{Sn(PTP)}_2$  (top and middle frames) the presence of the terpyridine ligands does not lead to any significant changes in the positions or intensities of the Q bands observed between  $\sim 550$  and  $\sim 620$  nm. The position of the Soret band (B band) at  $\sim 420$  nm is also unaffected, but its intensity is decreased. Similar reductions in the Soret-band intensity have been reported previously in some porphyrin complexes with axially or peripherally attached aryloxy or porphyrin groups<sup>35–38</sup> and have been interpreted as resulting from  $\pi-\pi$  interactions between the attached group and the porphyrin ring. Because a larger decrease in the Soret-band intensity is observed for  $\text{Sn(PTP)}_2$ , the spectra in Figure 3 suggest stronger  $\pi-\pi$  interactions in this compound. Another measure of these ligand–porphyrin interactions is provided by the NMR positions of protons of axially bound ligands, which experience an upfield shift that is induced by ring

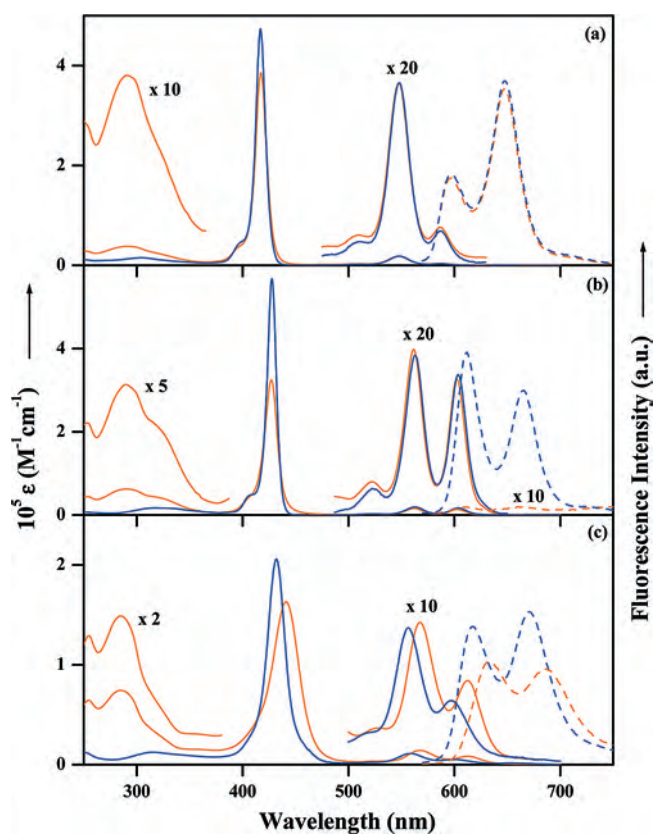


**Figure 3.** UV/vis absorption spectra (—) and fluorescence spectra (---) of (a)  $[\text{Al(OH)}]$  (blue) and  $\text{Al(PTP)}$  (orange), (b)  $[\text{Sn(OH)}_2]$  (blue) and  $\text{Sn(PTP)}_2$  (orange), and (c)  $[\text{P(OH)}_2]^+$  (blue) and  $[\text{P(PTP)}_2]^+$  (orange). The fluorescence spectra are of equimolar solutions ( $\sim 0.2$  o.d. at  $\lambda_{\text{exc}} = 555$  nm) in dichloromethane.

currents of the porphyrin.<sup>35,39</sup> In unbound hydroxyterpyridine, the phenyl protons that are ortho and meta to the oxygen

(35) Hirakawa, K.; Segawa, H. *J. Photochem. Photobiol., A* **1999**, *123*, 67–76.

(36) Susumu, K.; Kunimoto, K.; Segawa, H.; Shimidzu, T. *J. Photochem. Photobiol., A* **1995**, *92*, 39–46.

(37) Susumu, K.; Kunimoto, K.; Segawa, H.; Shimidzu, T. *J. Phys. Chem.* **1995**, *99*, 29–34.

(38) Maiya, G. B.; Krishnan, V. *J. Phys. Chem.* **1985**, *89*, 5225–5235.

(39) Hawley, J. C.; Bampos, N.; Abraham, R. J.; Sanders, J. K. M. *Chem. Commun.* **1998**, 661–662.

**Table 1.** Redox Potential Data in CH<sub>2</sub>Cl<sub>2</sub>, 0.1 M TBAP<sup>a</sup>

sample	potential ( $E_{1/2}$ ) V versus SCE		$E_{CT}(M^+PTP^-)$ (eV) <sup>b</sup>	$E_{CT}(M^-PTP^+)$ (eV)	$E_s$ (eV) <sup>c</sup>
	oxidation	reduction			
OH-PTP	1.00 <sup>d</sup>				3.76
[Al(OH)]	0.90, 1.45	-1.15, -1.55			2.13
Al(PTP)	0.96, 1.22, 1.57	-1.15, -1.56	>2.76	2.37	2.12
[Sn(OH) <sub>2</sub> ]	1.44	-0.92, -1.32			2.05
Sn(PTP) <sub>2</sub>	1.16	-0.86, -1.33	>2.96	2.02	2.05
[P(OH) <sub>2</sub> ] <sup>+</sup>		-0.52, -1.00			2.06
[P(PTP) <sub>2</sub> ] <sup>+</sup>	1.65	-0.39, -0.92	>3.60	2.04	2.01

<sup>a</sup> Error limits:  $E_{1/2}$ ,  $\pm 0.05$  V. <sup>b</sup> Based on the solvent limit of  $-1.8$  V for the reduction potential of PTP. <sup>c</sup> Estimated from the absorbance and fluorescence spectra. <sup>d</sup> Measured in DMSO, 0.1 M TBAP.

have chemical shifts of 6.89 and 7.74 ppm, respectively. In Al(PTP), these resonances are shifted upfield to 2.46 and 6.37 ppm, whereas in Sn(PTP)<sub>2</sub>, they occur at 1.99 and 6.28 ppm. Thus, the phenyl protons are shifted further upfield for Sn(PTP)<sub>2</sub> compared with Al(PTP). This shift is consistent with stronger  $\pi$ - $\pi$  interactions in the Sn complex but could also be the result of different inductive effects of the two metals. If the  $\pi$ - $\pi$  interactions are indeed stronger in the Sn complex, then the difference is probably due to the distortion of the Al complex with the central metal being pulled slightly out of the plane of the porphyrin ring by the terpyridine ligand,<sup>40</sup> whereas no such distortion is seen in the X-ray structure of Sn(PTP)<sub>2</sub>.

In contrast with Al(PTP) and Sn(PTP)<sub>2</sub>, the presence of the terpyridine ligands in [P(PTP)<sub>2</sub>]<sup>+</sup> leads to substantial broadening and a red shift of the porphyrin absorbance bands. Such effects have been observed as a result of strong  $\pi$ - $\pi$  interactions in the P porphyrin with axially ligated oxy-pyrene.<sup>35</sup> The ortho and meta proton chemical shifts (2.42 and 6.53 ppm, respectively) in [P(PTP)<sub>2</sub>]<sup>+</sup> lie downfield compared with those in the Al and Sn complexes, probably because of a weaker inductive effect from P rather than weaker  $\pi$ - $\pi$  interactions in the P porphyrin. To explain the broadening and the red shift in the absorbance spectrum of [P(PTP)<sub>2</sub>]<sup>+</sup>, one could postulate that the small size of the central P atom allows the distortion of the porphyrin ring, which promotes greater contact with the terpyridine ligand. Alternatively, the admixture of charge-transfer states may be greater in [P(PTP)<sub>2</sub>]<sup>+</sup> because its redox properties are different.

**Excited Singlet-State Properties.** The spectra in Figure 3 also allow the energy and photochemistry of the lowest excited singlet state to be investigated. The steady-state fluorescence spectra of the compounds measured with 555 nm excitation (porphyrin absorption) are shown as dashed curves in Figure 3 and are typical of penta- and hexacoordinated Al(III) and Sn(IV)/P(V) porphyrins, respectively.<sup>41-43</sup> Two aspects of these spectra are immediately apparent. First, the spectral shapes and the wavelengths of the emission maxima ( $\lambda_{em}$ ) of Al(PTP) and Sn(PTP)<sub>2</sub> are essentially the same as those of the corresponding hydroxy compounds, whereas a significant red shift of the emission is seen in

[P(PTP)<sub>2</sub>]<sup>+</sup>. This shift mirrors the shift in the Q-band absorption maxima and is probably due to the interaction of the phenyl terpyridine ligands and the porphyrin ring discussed above. Second, the fluorescence is strongly quenched in Sn(PTP)<sub>2</sub> and moderately quenched in [P(PTP)<sub>2</sub>]<sup>+</sup>, whereas no quenching is seen for Al(PTP). The quenching efficiency values are summarized in Table S1 in the Supporting Information. One possible explanation for the fluorescence quenching is that intramolecular charge transfer may depopulate the excited singlet state; the efficiency of this process depends on the nature of the metal/metalloid in the porphyrin.

This idea can be investigated by our estimating the relative energies of the various possible excited states. From the overlay of the absorption and fluorescence spectra shown in Figure 3, the energy of the lowest excited singlet state can be roughly estimated from the wavelength at which the absorbance and fluorescence spectra cross. For this estimation, the amplitudes of the absorption and emission spectra have been normalized such that the Q-band absorption maximum and the fluorescence maximum are the same. Note that in Figure 3 only the fluorescence spectra of the hydroxy compounds are plotted with this normalization and the relative amplitudes of the spectra of the terpyridine and hydroxy compounds have not been altered. The calculated energies are given in Table 1 as  $E_s$ , and for Al(PTP) and Sn(PTP)<sub>2</sub>, they are found to be close to those of the corresponding hydroxy porphyrins. For [P(PTP)<sub>2</sub>]<sup>+</sup>, the introduction of the PTP ligands appears to stabilize slightly the excited singlet state. Such behavior is consistent with the lowering of the  $\pi^*$  energy predicted by a simple two-level  $\pi$ - $\pi$  interaction scheme. However, it could also be interpreted as resulting from an admixture of a charge-transfer state to the excited singlet state.<sup>44</sup>

**Electrochemistry.** The redox midpoint potentials obtained from pulsed and cyclic voltammetry measurements can be used to estimate the energies of the possible charge-transfer states ( $E_{CT}$ ). Figure 4 shows the cyclic and differential pulse voltammograms of Al(PTP), Sn(PTP)<sub>2</sub>, and [P(PTP)<sub>2</sub>]<sup>+</sup> in CH<sub>2</sub>Cl<sub>2</sub> (0.1 M TBAP). The midpoint potentials obtained from the voltammograms are given in Table 1 along with those of the corresponding hydroxy compounds. As seen in Figure 4, each derivative undergoes two stepwise reduction reactions, and the associated midpoint potentials become increasingly negative on the order of Al(PTP) > Sn(PTP)<sub>2</sub>

(40) Davidson, G. J. E.; Tong, L. H.; Raithby, P. R.; Sanders, J. K. M. *Chem. Commun.* **2006**, 3087-3089.

(41) Kumar, P. P.; Maiya, B. G. *New J. Chem.* **2003**, 27, 619-625.

(42) Reddy, D. R.; Maiya, B. G. *J. Porphyrins Phthalocyanines* **2002**, 6, 3-11.

(43) Rao, T. A.; Maiya, B. G. *Inorg. Chem.* **1996**, 35, 4829-4836.

(44) Nagao, K.; Takeuchi, Y.; Segawa, H. *J. Phys. Chem. B* **2006**, 110, 5120-5126.

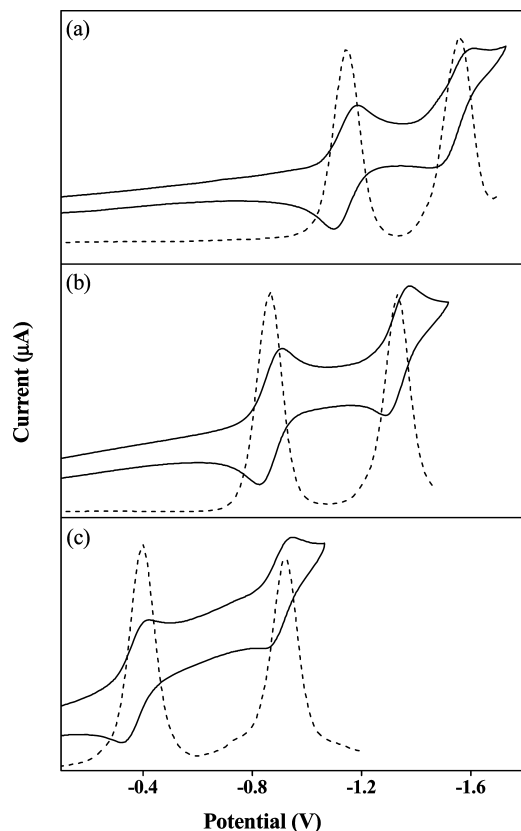


**Figure 4.** Cyclic (—) and differential pulse (---) voltammograms of (a) Al(PTP), (b) Sn(PTP)<sub>2</sub>, and (c) [P(PTP)<sub>2</sub>]<sup>+</sup> in CH<sub>2</sub>Cl<sub>2</sub>, 0.1 M TBAP (scan rate = 100 mV·s<sup>-1</sup>, modulation amplitude = 10 mV).

> [P(PTP)<sub>2</sub>]<sup>+</sup>. Wave analysis (from cyclic voltammetry) suggests that both of these electrode processes are reversible ( $i_{pc}/i_{pa} = 0.9–1.0$ ) and are diffusion-controlled ( $i_{pc}/\nu_{1/2}$  is constant in the scan rate ( $\nu$ ) range of 50–500 mV·s<sup>-1</sup> one-electron-transfer ( $\Delta E_p = 60–70$  and  $65 \pm 3$  mV for the Fc<sup>+</sup>/Fc couple) reactions.<sup>45</sup> We assign these reactions to successive one-electron additions to the porphyrin ring on the basis of a comparison to data for similar axial-bonding-type Al(III), Sn(IV), and P(V) porphyrins<sup>41–43</sup> and on the diagnostic criteria developed by Fuhrhop, Kadish, and Davis for porphyrin-ring reduction<sup>46</sup> ( $\Delta E_{1/2}$ , i.e., the difference in potential between the first one-electron and second one-electron addition is  $0.42 \pm 0.05$  V; see Table 1 where  $\Delta E_{1/2} = 0.40–0.53$  V). As expected, the midpoint potentials correlate with the oxidation number of the metal/metalloid in the porphyrin such that the higher the oxidation number, the more easily the porphyrin can be reduced.<sup>47</sup> The reduction of the terpyridine moiety was not observed because its midpoint potential is more negative than that of the solvent.

The anodic scan of Al(PTP) has three oxidation reactions, the first of which is reversible whereas the other two are irreversible (data not shown). On the basis of a comparison with the reference compounds OH-PTP and [Al(OH)], the first and third reactions are assigned to the oxidation of the porphyrin, whereas the second peak is assigned to the

oxidation of terpyridine. Sn(PTP)<sub>2</sub> shows a broad irreversible oxidation peak, which we assign to a combination of the first oxidation reactions of the terpyridine and porphyrin units. For [P(PTP)<sub>2</sub>]<sup>+</sup>, a single oxidation peak is observed. Because it is well known that P(V) porphyrins are difficult to oxidize,<sup>47–49</sup> we assign the peak to the oxidation of the terpyridine subunit. It has been well established<sup>46</sup> that for many different metal porphyrins  $E_{1/2}(\text{ox}) - E_{1/2}(\text{red})$  (i.e., the potential difference between the first ring oxidation and the first ring reduction) is in the range of  $(2.10–2.20) \pm 0.05$  V. If [P(PTP)<sub>2</sub>]<sup>+</sup> adheres to this rule, then the first one-electron oxidation would occur at a potential that is more positive than the solvent limit of ca. 1.8 V.

As can be seen in Table 1, the oxidation potential of terpyridine is shifted to a more positive value in the porphyrin complexes compared with that in OH-PTP. This shift can be rationalized as resulting from the electron-withdrawing effect of the metal/metalloid in the porphyrin and to the effect of  $\pi-\pi$  interactions in terpyridine. The shift is more pronounced in [P(PTP)<sub>2</sub>]<sup>+</sup> than in Al(PTP) or Sn(PTP)<sub>2</sub>, which is consistent with the high electronegativity of P(V) and the larger perturbation of the porphyrin UV/vis spectrum by the terpyridine ligands.

**Charge-Transfer State Energies.** Also shown in Table 1 are the energies of the possible charge-separated states calculated from the one-electron oxidation and reduction potentials of the porphyrin and terpyridine (i.e.,  $E_{CT}(\text{M}^+\text{PTP}^-) = E_{1/2}(\text{M}/\text{M}^+) - E_{1/2}(\text{PTP}/\text{PTP}^-)$  and  $E_{CT}(\text{M}^-\text{PTP}^+) = E_{1/2}(\text{PTP}/\text{PTP}^+) - E_{1/2}(\text{M}/\text{M}^-)$ , where M = Al(III), Sn(IV), and P(V) porphyrin). Clearly, electron transfer from terpyridine to the porphyrin is favored over the reverse process, particularly in the Sn and P complexes. A comparison with the estimated singlet-state energies of the porphyrins shows that light-induced electron transfer to terpyridine is not feasible but in the Sn and P porphyrins the energy of the charge-separated state in which an electron is transferred from terpyridine to the porphyrin is similar to that of the excited singlet state. The calculated energies of the charge-transfer states do not include the electron–hole stabilization. The magnitude of this effect is difficult to quantify, but it lowers the energy of the charge-transfer states relative to that of the excited singlet state, making electron transfer from the terpyridine to the porphyrin more exergonic. Thus the fluorescence quenching and the electrochemical data suggest that for Sn(PTP)<sub>2</sub> and [P(PTP)<sub>2</sub>]<sup>+</sup> the excited singlet state of the porphyrin is depopulated by electron transfer from the HOMO of the terpyridine ligand into the half-filled HOMO of the porphyrin. To test this hypothesis, we have measured the fluorescence lifetimes associated with the excited singlet state.

**Time-Resolved Fluorescence Spectroscopy.** A comparison of the fluorescence decay profiles is shown in Figure 5, and the decay lifetimes obtained by fitting either a mono- or biexponential decay function to the experimental curves are summarized in Table 2. As expected, the fluorescence decay of Al(PTP) is virtually identical to that of the corresponding

(45) Nicholson, R. S.; Shain, I. *Anal. Chem.* **1964**, *36*, 706–723.

(46) Fuhrhop, J. H.; Kadish, K. M.; Davis, D. G. *J. Am. Chem. Soc.* **1973**, *95*, 5140–5147.

(47) Marrese, C. A.; Carrano, C. J. *Inorg. Chem.* **1983**, *22*, 1858–1862.

(48) Marrese, C. A.; Carrano, C. J. *Inorg. Chem.* **1984**, *23*, 3961–3968.

(49) Kadish, K. M. *Prog. Inorg. Chem.* **1986**, *34*, 435–605.

**Table 2.** Fluorescence Lifetime Data,  $\lambda_{\text{exc}} = 406 \text{ nm}^a$ 

sample	$\lambda_{\text{em}}$ (nm)	$\tau$ , ns ( $A$ ) <sup>a</sup>		
		DCM	ACN	DMSO
[Al(OH)]	600	5.09	5.95	6.01
Al(PTP)		5.17	5.77	6.01
[Sn(OH) <sub>2</sub> ]	610	1.38	1.56	1.49
Sn(PTP) <sub>2</sub>		1.43 (2%), 0.488 (98%)	2.14 (9%), 0.525 (91%)	1.24 (28%), 0.504 (72%)
[P(OH) <sub>2</sub> ] <sup>+</sup>	620	3.70	4.38	4.18
[P(PTP) <sub>2</sub> ] <sup>+</sup>		2.32 (81%), 1.63 (19%)	3.08 (38%), 1.41 (62%)	3.01 (42%), 1.52 (58%)

<sup>a</sup> Error limits:  $\tau \pm 10\%$ .  $A$  is the relative amplitude of the decay components.

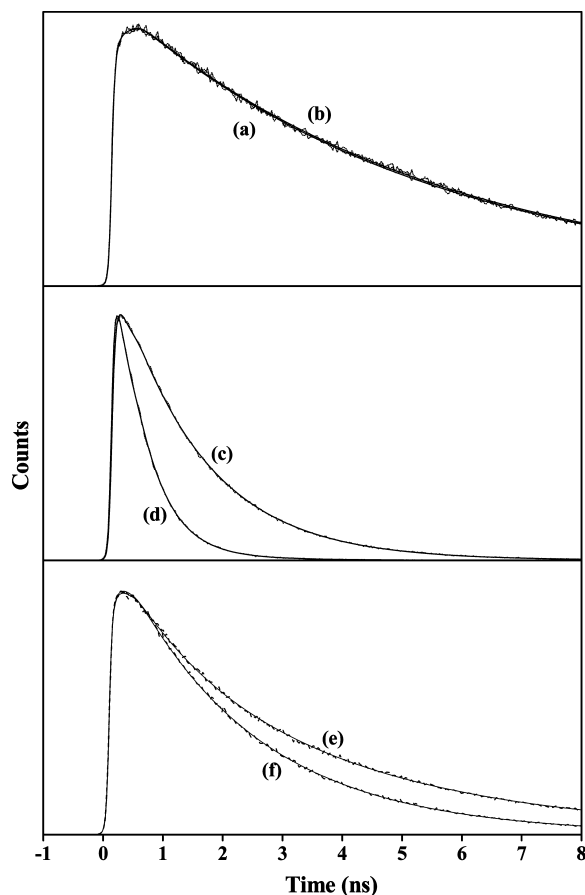


**Figure 5.** Time-resolved fluorescence decay profiles of (a) [Al(OH)], (b) Al(PTP), (c) [Sn(OH)<sub>2</sub>], (d) Sn(PTP)<sub>2</sub>, (e) [P(OH)<sub>2</sub>]<sup>+</sup>, and (f) [P(PTP)<sub>2</sub>]<sup>+</sup> in dichloromethane. The full thin lines are fits to the experimental decays.

hydroxy compound, whereas a considerable decrease in the lifetime is seen for Sn(PTP)<sub>2</sub> and [P(PTP)<sub>2</sub>]<sup>+</sup>. For the latter two compounds, the decay also becomes biexponential. The origins of the two kinetic components are not immediately apparent, but they could be due to different conformations of the complex with different quenching efficiencies, that is, with different rates of electron transfer. Regardless of this, the time-resolved fluorescence results show that the fluorescence quenching is accompanied by a decrease in the fluorescence lifetime.

**Transient Absorbance Spectroscopy.** In an attempt to determine whether the fluorescence quenching in Sn(PTP)<sub>2</sub> and [P(PTP)<sub>2</sub>]<sup>+</sup> is due to electron transfer, we have performed transient absorbance experiments in the visible region on Al(PTP), Sn(PTP)<sub>2</sub>, [P(PTP)<sub>2</sub>]<sup>+</sup>, and their hydroxy analogues (M. Wasielewski and V. Gunderson, unpublished results). However, the difference spectrum of the reduced porphyrin

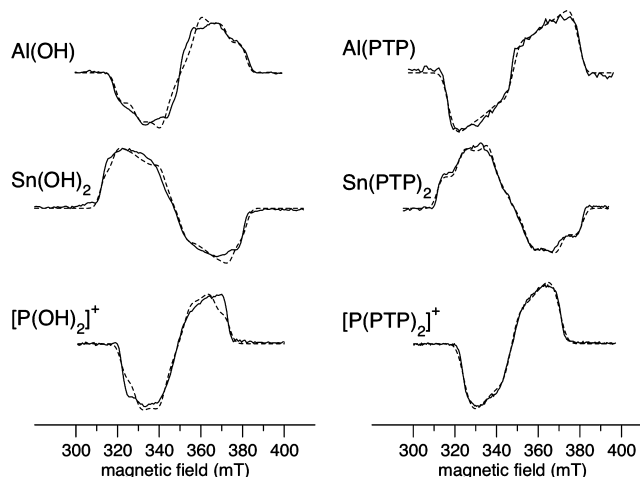


**Figure 6.** Low-temperature TREPR spectra of Al(PTP), Sn(PTP)<sub>2</sub>, and [P(PTP)<sub>2</sub>]<sup>+</sup> and the corresponding hydroxy compounds in the liquid crystal 5CB. The samples were frozen in the absence of any external fields and are not macroscopically ordered. The experimental spectra taken at 80 K (—) are shown along with simulated spectra (---).

is nearly identical to that of triplet state,<sup>19</sup> and absorbance differences due to the formation of the terpyridine cation are not predicted to occur in the visible region. Thus, the charge-separated state is difficult to distinguish from the triplet state, and the origin of the fluorescence quenching remains ambiguous.

**Transient Electron Paramagnetic Resonance Spectroscopy.** The presence of light-induced radical pairs is most easily demonstrated by TREPR spectroscopy. The X-band spin-polarized TREPR spectra of Al(PTP), Sn(PTP)<sub>2</sub>, and [P(PTP)<sub>2</sub>]<sup>+</sup> and their hydroxy analogues are presented in Figures 6–8. Figure 6 shows the spectra measured at 80 K. Under these conditions, the terpyridine complexes and their hydroxy analogues have nearly identical spectra, which are readily assigned to the triplet state of the porphyrin populated by spin–orbit-coupling-induced intersystem crossing (isc). The spectra are well simulated on this basis (dashed curves) using an approach that is described in detail elsewhere.<sup>27,50,51</sup> Briefly, the spin polarization is calculated as the traceless diagonal part of the reduced density matrix for the triplet state  $\Delta\rho$  that we write as a linear combination of contributions of different symmetries. Spin–orbit coupling isc produces multiplet polarization that is described by two terms that follow the internal symmetry of the molecule

(50) Kandrashkin, Y. E.; Asano, M. S.; van der Est, A. *J. Phys. Chem. A* **2006**, *110*, 9607–9616.

(51) Kandrashkin, Y. E.; Asano, M. S.; van der Est, A. *J. Phys. Chem. A* **2006**, *110*, 9617–9626.

$$\Delta\rho_{m,\parallel} = \frac{3}{2}(\cos^2\theta - 1/3)\left(S_z^2 - \frac{1}{3}\vec{S}^2\right)$$

$$\Delta\rho_{m,\perp} = \frac{3}{2}\sin^2\theta \cos 2\varphi\left(S_z^2 - \frac{1}{3}\vec{S}^2\right) \quad (1)$$

where  $\theta$  and  $\phi$  describe the orientation of the magnetic field relative to the molecular axes. Radical pair recombination to a molecular triplet state can also generate multiplet polarization that is described by the spin operators in the laboratory frame of reference

$$\Delta\rho_{m,\text{lab}} = S_z^2 - \frac{1}{3}\vec{S}^2 \quad (2)$$

Both of these processes also produce net polarization in the triplet state. This polarization is generally quite weak, and here, we assume that the orientation dependence of this contribution can be ignored. In this case, it is given by

$$\Delta\rho_n = S_z \quad (3)$$

We write the total population distribution as a weighted sum of these four contributions

$$\Delta\rho \propto \kappa_{m,\parallel}\Delta\rho_{m,\parallel} + \kappa_{m,\perp}\Delta\rho_{m,\perp} + \kappa_{m,\text{lab}}\Delta\rho_{m,\text{lab}} + \kappa_n\Delta\rho_n \quad (4)$$

and treat the weighting coefficients  $\kappa_{m,\parallel}$ ,  $\kappa_{m,\perp}$ ,  $\kappa_{m,\text{lab}}$ , and  $\kappa_n$  as adjustable parameters. The values of the parameters used in the simulations in Figures 6–8 are given in Table 3. As can be seen in Table 3, all of the spectra taken at 80 K are described using essentially only the parameter  $\kappa_{m,\parallel}$ , which is expected for a spin–orbit coupling *isc* in a molecule with approximately 4-fold symmetry. The sign of the polarization is inverted in the Sn compounds because the in-plane components of the spin–orbit coupling is dominant, whereas the out-of-plane component is dominant for the Al and P porphyrins. This difference is not unexpected because Sn is a much heavier element than Al or P and should make a greater contribution to the overall spin–orbit coupling.<sup>52</sup> The Sn porphyrins also have slightly broader triplet spectra than the Al and P porphyrins, and they show the net absorptive polarization (Figure 6, middle; Figure 8, bottom left). As discussed by Salikhov et al.,<sup>53</sup> the net polarization generated during *isc* is approximately proportional to the zero-field splitting parameter  $D$ , which contains a contribution from spin–orbit coupling. Thus, the net polarization and larger  $D$  values imply stronger spin–orbit coupling, as would be expected with a heavier central metal such as Sn in the porphyrin.

Figure 7 shows corresponding room-temperature data for  $[\text{P}(\text{PTP})_2]^+$  measured in a partially oriented liquid-crystalline solvent. As can be seen, two sequential spin-polarized TREPR spectra are observed. The first is consistent with the triplet state of a radical pair, whereas the latter is assigned to the triplet state of the porphyrin formed by charge recombination. An analysis of the EPR time traces yields a lifetime of  $\sim 175$  ns for the radical pair. On the basis of the

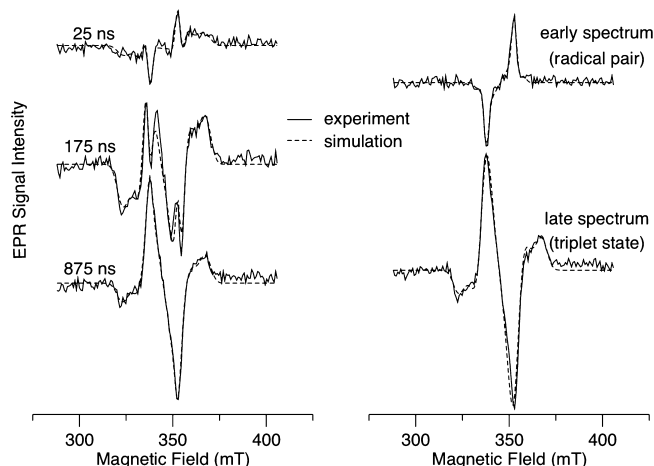


**Figure 7.** Room-temperature TREPR spectra of  $[\text{P}(\text{PTP})_2]^+$  in the liquid crystal E7. The spectra on the left have been extracted from the complete time/field data set at the times indicated. The data set can be decomposed into the two sequential spectra shown on the right, as described by Kandrashkin et al.<sup>27</sup> The early spectrum is assigned to the triplet state of the radical pair  $^3(\text{PTP}^+\text{P}^-)$ . The late spectrum is assigned to the triplet state of P porphyrin  $^3\text{P}$ . The parameters used in the simulations are given in Table 3.

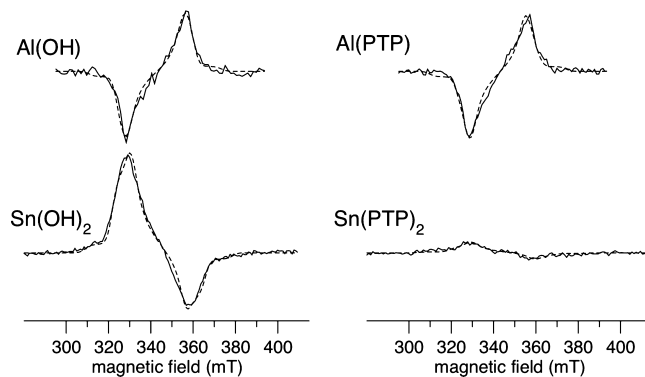


**Figure 8.** Room-temperature TREPR spectra of the porphyrin complexes Al(PTP), Al(OH), Sn(PTP)<sub>2</sub>, and Sn(OH)<sub>2</sub> in the liquid crystal 5CB. The spectra represent the signal intensity in a time window that is 200 ns wide and centered at 300 ns following the laser flash. The parameters used in the simulations (---) are given in Table 3.

spectroscopic and redox properties of the terpyridine and porphyrin moieties discussed above, we have proposed<sup>27</sup> that the radical pair is formed by electron transfer from the terpyridine to the excited P(V) porphyrin. The fact that at low temperature the radical-pair spectrum is not observed and the spin-polarization pattern of the porphyrin triplet is dramatically different is explained by postulating that the electron transfer is inhibited at low temperature because the molecular motion is required to stabilize the radical pair. We propose that in the absence of this stabilization the porphyrin triplet state is populated via spin–orbit-coupling-mediated *isc* from the excited singlet state. The fluorescence quenching and lifetime data discussed above suggest that altering the redox potential of the porphyrin changes the efficiency of the electron transfer such that it does not occur in Al(PTP). Figure 8 shows a comparison of the room-temperature TREPR spectra of Al(PTP) and Sn(PTP)<sub>2</sub> and the corresponding hydroxy compounds. Consistent with the optical data, the room-temperature spectrum of Al(PTP) is virtually identical to that of [Al(OH)]. The simulations of

(52) Gouterman, M.; Schwarz, F. P.; Smith, P. D.; Dolphin, D. *J. Chem. Phys.* **1973**, *59*, 676–690.

(53) Salikhov, K. M.; Sagdeev, R. Z.; Buchachenko, A. L. *Spin Polarization and Magnetic Effects in Radical Reactions*; Molin, Y. N., Ed.; Elsevier: Amsterdam, 1984.

**Table 3.** Magnetic Parameters of Axially Linked Terpyridine Porphyrins and Corresponding Hydroxy Compounds<sup>a</sup>

sample temperature (K)	ZFS parameters (mT)		line width (mT) <sup>b</sup>	order parameters		weighting parameters <sup>c</sup>			
	<i>D</i>	<i>E</i>		<i>S<sub>zz</sub></i>	<i>S<sub>xx</sub> - S<sub>yy</sub></i>	<i>κ<sub>m,  </sub></i>	<i>κ<sub>m,⊥</sub></i>	<i>κ<sub>m,lab</sub></i>	<i>κ<sub>n</sub></i>
[Al(OH)] 295 K	29	1.54	2.3	-0.2	0	-1.0	0.0		0.02
80 K	29	4	2.3	0	0	-1.0	0.04		0.0
Al(PTP) 295 K	30	28	2.3	-0.2	0	-1.0	0.17		0.04
80 K	30	8	2.3	0	0	-1.0	-0.08		-0.02
[Sn(OH) <sub>2</sub> ] 295 K	33	3	2.3	-0.2	0	1.0	-0.04		-0.12
80 K	33	7	2.3	0	0	1.0	0.10		-0.03
Sn(PTP) <sub>2</sub> 295 K	33	3	2.3	0.3	0.3	1.0	0.47	-0.67	-0.05
80 K	33	5	2.3	0	0	1.0	0.02		-0.07
[P(OH) <sub>2</sub> ] <sup>+</sup> 295 K	24	3	2	-0.2	0	-1.0	0.6		
80 K	26	4	2	0	0	-1.0	-0.05		0.06
[P(PTP) <sub>2</sub> ] <sup>+</sup> 295 K	14	1	1	0.3	0	-0.53	1.0	0.41	
triplet 295 K	24	2.5	2.5	0.3	0.3	-0.58	-1.0	0.49	0.02
80 K	24	4	2.3	0	0	-1.0	-0.07		

<sup>a</sup> The estimated error in the ZFS parameters is  $\pm 0.5$  mT. The values in magnetic field units are related to frequency units by  $g\beta/h = 28.024$  MHz/mT.

<sup>b</sup> Gaussian half-width. <sup>c</sup> The parameters  $\kappa_{m,||}$  and  $\kappa_{m,\perp}$  are related to the population rate parameters associated with the three molecular axes (see, e.g., ref 58) as follows:  $\kappa_{m,||} = 1.0$  and  $\kappa_{m,\perp} = 0.0$  correspond to  $P_x/P_y/P_z = 0:0:1$ ;  $\kappa_{m,||} = -1.0$  and  $\kappa_{m,\perp} = 1.0$  correspond to  $P_x/P_y/P_z = 0:1:0$ , and  $\kappa_{m,||} = -1.0$  and  $\kappa_{m,\perp} = -1.0$  correspond to  $P_x/P_y/P_z = 1:0:0$ .

the spectra (dashed curves in Figure 8, parameters in Table 3) show that both spectra are due to the triplet state of the porphyrin populated by *isc*. For Sn(PTP)<sub>2</sub> (Figure 8, bottom right), essentially no spin-polarized EPR spectrum is seen at room temperature. There is some indication of a very weak spectrum from the triplet state, and we have attempted to simulate it, but the parameters obtained are probably not meaningful given the poor signal/noise ratio of the experimental data. The strong fluorescence quenching for this compound and the faster fluorescence decay time and the redox potentials are consistent with the radical-pair formation. However, the TREPR data show that if this interpretation is correct then the radical pair is not EPR-detectable. Such behavior would be expected if its lifetime was shorter than the spectrometer response time and if the decay pathway was predominantly via the singlet state of the radical pair. A balance between the rate of singlet–triplet mixing in the radical pair and the rates of singlet and triplet recombination governs the decay pathway of the charge-separated state. Hence, a shift in any one of these parameters can lead to a change in the radical-pair lifetime and the relative yield of triplet and singlet recombination. It is likely that the recombination rates and the rate of singlet–triplet mixing are similar in our system, in which case both singlet and triplet recombination probably occur in the Sn and P complexes. Under these conditions, a slight increase in the singlet recombination rate would be expected to cause a decrease in the overall lifetime of the radical pair and the yield of triplet recombination. From Table 1, the free-energy change ( $\Delta G^\circ$ ) for charge recombination is 20 mV lower for Sn(PTP)<sub>2</sub> than for [P(PTP)<sub>2</sub>]<sup>+</sup>. If the recombination reaction lies in the inverted region, then this difference would lead to a slightly higher rate of singlet recombination to the ground state. However, given the relatively small energy difference between the radical pair and the excited singlet state, it is likely that singlet recombination occurs via the excited singlet state. It is important to note here that the radical-pair lifetime in the P compound (175 ns) is close to the time resolution of the spectrometer ( $\sim 100$  ns), thus a relatively small change in the radical-pair lifetime would put it below the time resolution of the instrument. Hence even a modest decrease

in the radical-pair lifetime of Sn(PTP)<sub>2</sub> compared with that of [P(PTP)<sub>2</sub>]<sup>+</sup> could make it undetectable. Alternatively, the possibility that the rapid spin relaxation could make the radical pair and triplet state undetectable cannot be ruled out.

## Discussion

Figure 9 shows an energy-level diagram and kinetic scheme based on the electrochemical and spectroscopic data presented above. The energies of the possible charge-separated state calculated from the midpoint potentials show that in all three cases electron transfer from the porphyrin to the terpyridine is energetically very unfavorable. However, the  $\Delta G^\circ$  values for electron transfer from terpyridine to the porphyrin in CH<sub>2</sub>Cl<sub>2</sub> are estimated to be 0.25, -0.03, and 0.03 eV for Al(PTP), Sn(PTP)<sub>2</sub>, and [P(PTP)<sub>2</sub>]<sup>+</sup>, respectively. In keeping with these energies, no fluorescence quenching or radical pair TREPR spectrum is observed for Al(PTP), whereas steady-state fluorescence quenching, a decrease in the fluorescence decay lifetimes, and TREPR spectra that are indicative of electron transfer are observed for Sn(PTP)<sub>2</sub> and [P(PTP)<sub>2</sub>]<sup>+</sup>. The most straightforward explanation of these observations is that electron transfer from terpyridine to the HOMO of the porphyrin in its excited singlet state occurs in Sn(PTP)<sub>2</sub> and [P(PTP)<sub>2</sub>]<sup>+</sup>. In this regard, we note that recent fluorescence studies of axial-bonding-type Al(III) porphyrin-based dyads and triads<sup>41</sup> on bisaxially ligated aryloxo derivatives of Sn(IV) porphyrins<sup>42,54</sup> or P(V) porphyrins<sup>35,36,43,44</sup> have indicated that the relaxation of the singlet excited states of these complexes involves a significant contribution from the ligand-to-porphyrin charge-transfer states. For Sn(PTP)<sub>2</sub>, it is important to note that whereas the data support the idea of electron transfer from terpyridine to the excited porphyrin there is no direct evidence of the presence of the charge-separated state in this compound. Alternatively, it could be argued that the quenching of the excited singlet state might occur via an enhanced internal conversion or via metal-to-porphyrin charge-transfer states that have been suggested to mix strongly with the Q-band

(54) Giribabu, L.; Rao, T. A.; Maiya, B. G. *Inorg. Chem.* **1999**, *38*, 4971–4980.

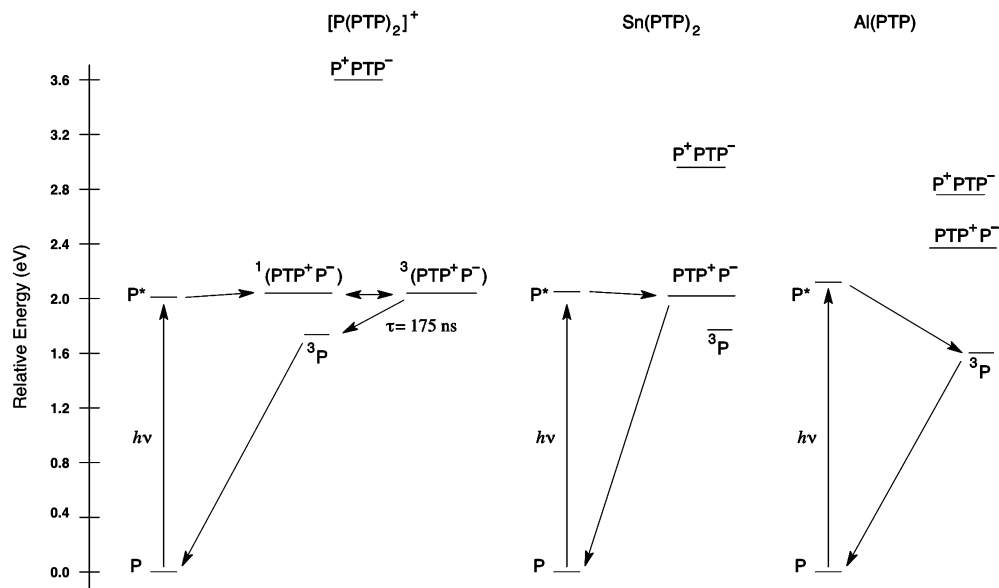


**Figure 9.** Approximate energy-level diagram for the complexes  $[P(PTP)_2]^+$ ,  $Sn(PTP)_2$ , and  $Al(PTP)$  based on measured redox midpoint potentials and UV/visible absorption and emission data. The estimated energies of the excited singlet states and charge-transfer states are given in Table 1. The energies of the triplet states have been calculated from the wavelength of the phosphorescence maxima of related porphyrins.<sup>52,56,57</sup>

transitions in  $Sn$  porphyrins. Such mechanisms are possible, but the fact that a strong spin-polarized triplet spectrum is observed at low temperature argues in favor of the formation of a solvent-reorganization-stabilized radical pair as the most likely source of the quenching at room temperature.

The estimated  $\Delta G^\circ$  values indicate that the driving force for electron transfer is small. These values have a considerable uncertainty associated with them because the electron-hole stabilization has not been taken into account and they are also solvent-dependent. Hence, they could be significantly different under the conditions used for some of the experiments. It is reasonable to assume that the magnitude of the reorganization energy,  $|\lambda|$ , is probably considerably larger than that for  $|\Delta G^\circ|$  in this reaction. In general, the reorganization energy can be divided into two contributions:  $\lambda_i$ , which arises from the internal motion of the molecule, and  $\lambda_s$ , which is due to the reorganization of the solvent.<sup>16,55</sup> The latter contributes to the overall driving force of the reaction. At low temperature when the solvent is frozen, the stabilization due to the solvent is no longer available, and the effective driving force is smaller. Given the small estimated values of  $|\Delta G^\circ|$  in these systems, it is reasonable to expect that electron transfer would not be viable in a frozen solution. In agreement with this expectation, the TREPR data show no evidence of radical-pair formation for any of the complexes at low temperature.

If the fluorescence quenching, decreased fluorescence lifetimes, and radical pair TREPR spectrum are indeed due to electron transfer from terpyridine to the excited porphyrin, then this implies that the efficiency of this process can be modulated by altering the metal/metalloid in the porphyrin.

In both  $[P(PTP)_2]^+$  and  $Sn(PTP)_2$ , the charge-separated state is estimated to be similar in energy to the lowest excited singlet state. In addition, the parameters obtained by fitting the spin-polarization patterns of  $[P(PTP)_2]^+$  indicate that the radical-pair triplet state is populated by a mechanism such as spin-orbit coupling that follows the internal symmetry of the molecule. As discussed above, the UV/vis spectrum of  $[P(PTP)_2]^+$  suggests that the small energy gap between the excited singlet state and the radical pair promotes the mixing of these two states. In such a case, the charge separation occurs to some extent directly upon excitation, and the transition from the excited singlet state to the radical-pair triplet requires a certain amount of isc character. Consistent with this idea, the polarization patterns show a mixture of contributions that follow the laboratory frame, resulting from singlet-triplet mixing in the radical pair, and, following the molecular symmetry, resulting from spin-orbit-coupling-mediated isc.

## Conclusions

Here, we have demonstrated the importance of the oxidation number of the central metal/metalloid in controlling electron transfer to a series of porphyrins from axially bound terpyridine. Understanding this dependence is a necessary prerequisite to designing complexes in which a strong oxidizing potential is generated in a metal center by light-induced electron transfer to an attached chromophore. Our data also suggest that solvent reorganization is important in the stabilization of the light-induced electron-transfer states for this series of molecules. The ability of P porphyrin to photo-oxidize terpyridine and to form a radical pair at a relatively long distance makes this species a promising candidate as a model for the bacterial reaction center  $P_{680}$ . We are now extending these studies to test whether it is able to oxidize Mn coordinated by terpyridine. However, even if this reaction is possible, then many additional challenges

(55) Chen, P. Y.; Meyer, T. J. *Chem. Rev.* **1998**, *98*, 1439–1477.

(56) Harriman, A.; Osborne, A. D. *J. Chem. Soc., Faraday Trans.* **1983**, *79*, 765–772.

(57) Sayer, P.; Gouterman, M.; Connell, C. R. *J. Am. Chem. Soc.* **1977**, *99*, 1082–1087.

(58) Levanon, H. *Rev. Chem. Intermed.* **1987**, *8*, 287–320.

remain. First, the anion generated by the ligand-to-porphyrin electron transfer must be stabilized. Ultimately, an external electron scavenger must be used, but a secondary acceptor such as a quinone attached to the porphyrin may also be necessary to stabilize the charge-separated state.

**Acknowledgment.** This work was supported by the Natural Sciences and Engineering Research Council of Canada. Financial support from the CSIR (New Delhi, India) and the Board of Research in Nuclear Sciences (Mumbai,

India) is also gratefully acknowledged. We thank UGC & CSIR (India) for research fellowships.

**Supporting Information Available:** Experimental procedures and synthesis; absorbance and fluorescence data; NMR spectra; X-ray crystal structure details; X-ray structure and crystal packing; and selected bond lengths and angles. This material is available free of charge via the Internet at <http://pubs.acs.org>.

IC702480M